

gas content. Volcanic craters are connected by magma pipes with magma chambers. The internal dynamics of the volcano must be monitored for its physical parameters continuously so that early symptoms of an eruption can be detected, during and after the eruption. Due to the presence of magma pipes and chambers beneath the earth, their physical parameters can give rise to a measurable potential field at the earth's surface. Pipes and magma chambers do not have to be cylindrical pipes and spherical pockets but can form of dykes with many branches. The internal structure of a volcano can be modeled using a combination of gravitational, magnetic, electromagnetic, and seismic methods.

The combination of gravitational acceleration measurements with a gravity measuring instruments and accurate positioning with DGPS around volcanic areas is repeated from year to year. Correlation analysis will produce four types of combination results:

- If gravity rises and the position of the observation point rises, it can be interpreted as increasing magma.
- If gravity increases and the position of the observation point -significantly decreases can be interpreted as a fixed mass and position of magma and slopes of descending volcanoes or subsidence.
- If gravity goes down and the position of the observation point goes up, it can be interpreted that the mass and position of the magma are fixed, and the slopes of the volcano are expanding up.
- If gravity decreases and the position of the observation point decreases, it can be interpreted as a decrease in magma mass accompanied by the collapse of the mountain slopes.

Repeated gravity surveys will be useful for studying deformation in volcanoes and have the added advantage of providing information about changes in subsurface mass. Volcanic monitoring using the gravity method is carried out by observing changes in gravity (Δg) to changes in altitude (Δh) at observation points on gravity data for Merapi Volcano in 2018 and 2019, conducted by the team from the Center for Research and Development of Geological Disaster Technology (BPPTKG) Yogyakarta and Kelud Volcano gravity data for the 2019 survey. In the late 20th and early 21st centuries, Mount Merapi erupted every 2-5 years. Most eruptions have low to moderate explosive power with Volcanic Explosivity Index (VEI). Based on the history of the merapi eruption [1], the eruption occurred on 11 May 2018 which produced an eruptive column 5.5 km above the summit (Venzke, 2018). This pyroclastic flow descends the slope at a speed of 200-300 km/h and has a temperature of 200-300°C [1], [2]. Volcano systems generally consist of four zones, including supply system, storage system, transport system, and eruptive system [3].

The lift caused by the addition of an infinitely flat horizontal slab with material density and thickness h is called the gravitational slab effect given by: $g = 2\pi G\rho h$. In this case, the ratio of the change in gravity to the change in altitude at a given station $\Delta g/\Delta h$ is

the combination of the free air effect and the Bouguer effect [4]:

$$\frac{\Delta g}{\Delta h} = (-3.08672 + 2\pi\rho G) \mu\text{Gal}/\text{cm} \quad (1)$$

Δg = change in gravity, Δh = change in height, ρ = density, G = of universal gravity constant = $6.67 \times 10^{-11} \text{ kg}^{-1}\text{m}^3\text{s}^{-2}$ in the field of volcanology the infinite horizontal slab model is suitable for intrusion, while for spherical may be more suitable for shallow magma reservoirs. In this case, the Bouguer gradient is given by [5], [6]:

$$\frac{\Delta g}{\Delta h} = \left(-3.08672 + \frac{4\pi\rho G}{3}\right) \mu\text{Gal}/\text{cm} \quad (2)$$

The method used to estimate the internal activity of a volcano is to use a graph of g against h (Figure 1), which illustrates the relationship between changes in gravity and changes in altitude for several source models. Lines with negative gradients correspond to the gradient of free air, $-3.086 \text{ Gal}/\text{cm}$, which is true in the case of no change in mass, and to plates or spheres with: $\rho = 2.3 \text{ gr}/\text{cm}^3$. The line with a positive gradient represents the change in the corrected gravity of free air ($\Delta g'$), which is the difference between the change in gravity measured and the gravitational gradient of free air [7], [8]:

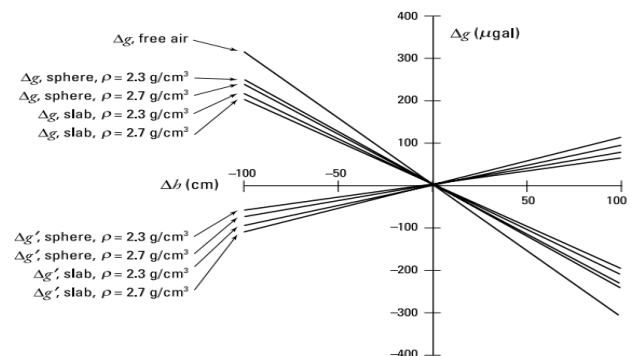


Figure 1 The relationship between gravity changes and elevation changes for several models [9]

2.0 METHODOLOGY

The research location is in the top of Merapi Volcano (Figure 2) and the top of Kelud Volcano area to the slopes (Figure 3). The Merapi gravity data used is the gravity data of the Geological Disaster Technology Research and Development Center (BPPTKG), Yogyakarta [6]. The measurement of gravity values was carried out in April 2018 and March 2019 in the Merapi area as many as nine measurement points. The data consists of the observed gravity value, the coordinates of the measurement point and the altitude data. For the measurement of the height of the observation point, only the first measurement was carried out (April 2018). The measurement point is in

the form of a profiling in the NS direction with a distance between points of ± 500 m.

In the process of migrating from the magma source to the surface, the magma enters the reservoir zone. In Merapi, there are two zones of magma chamber, including shallow and deep magma chamber. The existence of shallow reservoirs is present at depths of 1.5-2.5 km based on seismic modeling [10], [11], and 0.8-1.8 km from the peak based on gravitational modeling [12].

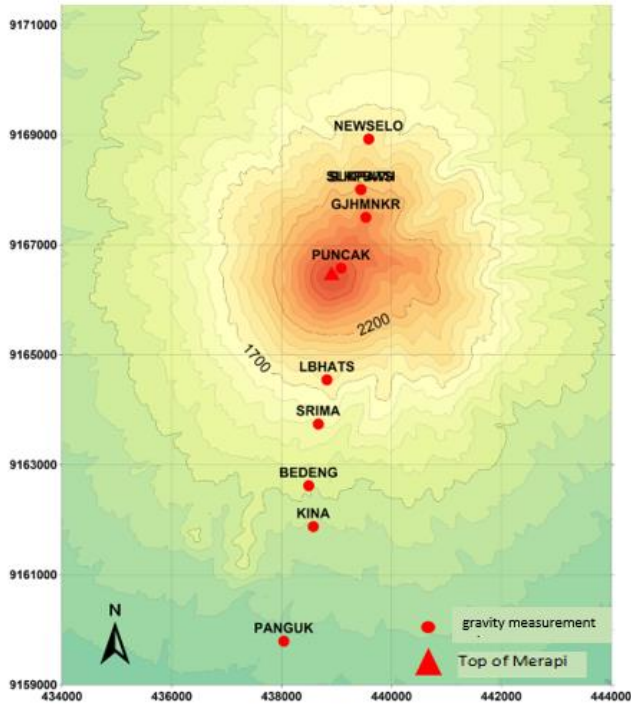


Figure 2 Location of the gravity measurement points (red point) at the top of Merapi Volcano

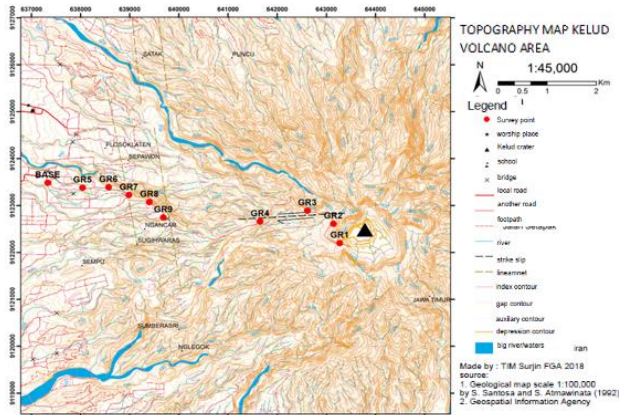


Figure 3 Location of gravity measurement points (red point) at the top of Kelud Volcano [13]–[15]

The base station used is at the BPPTKG Yogyakarta office with the international number g 114072 at coordinates $7.8^{\circ}\text{S } 110.405^{\circ}\text{E}$. In addition, this study also uses the National Digital Elevation Model (DEMNAS) data with a spatial resolution of 0.27 arc-

sec or 8.158 m. This DEM data can be downloaded on the website of the Geospatial Information Agency (www.tides.big.go.id). The data on the gravity and height of Kelud Volcano were taken on July 15-16 2019, there are ten measurement points with a base station at the Kelud Volcano Observation Post, Margomulyo Village, Wates District, Kediri, at coordinates $08^{\circ} 55' 40.14''$ South Latitude and $112^{\circ} 14' 45.48''$ East Longitude, elevation 675 above sea level [16].

2.1 Data Processing

Gravity observations are obtained after correcting tool height, correcting tides, and correcting drift. Complete Bouguer Anomaly Gravity values were obtained after correcting for latitude, free air, Bouguer (infinity slab and spherical) and terrain effects. Each observation point is calculated the difference in the value of the complete Bouguer anomaly g to the reference point (top of station), which is stated in equation 3 [17].

$$\Delta g_i = \Delta g_{ABL_i} - \Delta g_{ABL_{reference}} \tag{3}$$

Where Δg_i is the complete Bouguer anomaly difference at the i -th point, Δg_{ABL_i} is the complete Bouguer anomaly value at the i -th point, $\Delta g_{ABL_{reference}}$ is the complete Bouguer anomaly at the reference point (top of station). Similar process is done for the elevation of the observation point. The obtained elevation value is calculated by calculating the elevation difference h , including [18]:

$$\Delta h = h_i - h_{reference} \tag{4}$$

where Δh_i Δh_i is the difference between the elevation of the i -th point and the reference point, h_i is the elevation of the i -th point, $h_{reference}$ is the elevation of the reference point (top of station). Then the values of Δg and Δh will be plotted on the Δg versus Δg graph [19].

2.2 Data Analysis

The complete Bouguer anomaly changes with altitude are caused by internal effects occurring within the body of the volcano. The mathematical pattern approach of these changes can characterize the internal activity of the volcano. The analysis of the slope or gradient of the regression line $\Delta g_{obs}/\Delta h$ is done by comparing the regression values obtained. In Turcotte and Schubert (2014), it is explained that the change in the slope of the regression line shows a change in the density value to the value of the theoretical free air gradient line. If the line gradient is getting bigger then the density value is getting smaller but if the gradient value is getting smaller then the density value is getting bigger. The regression line changes refer to the theoretical regression lines of FAG

(Free air gradient) and BCFAG (Bouguer Correction-Free Air Gradient).

3.0 RESULTS AND DISCUSSION

3.1 Graph of Δg_{obs} against h

Each g_{obs} value and elevation h of the observation point is subtracted from the value at the highest observation point (Peak station). The difference is called g_{obs} and h (Figure 4).

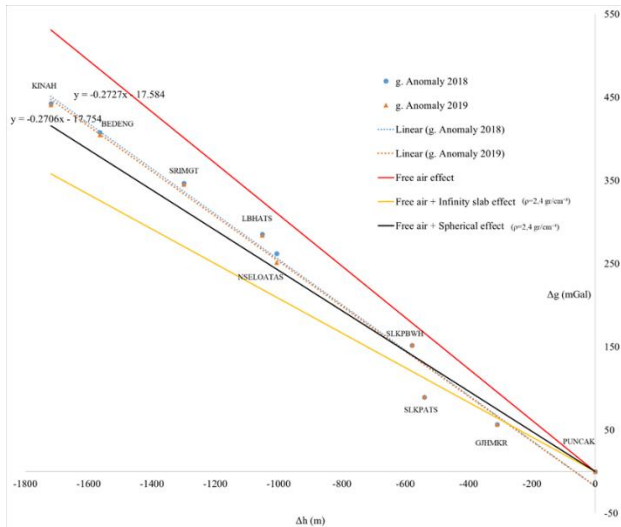


Figure 4 Graph of Δg_{obs} against Δh of Mount Merapi Volcano in 2018 and 2019

The results of the processing of the observed gravitational field are further processed to determine the gradient of $g_{obs}/\Delta h$. A significant change in $\Delta g_{obs}/\Delta h$ occurred at New Selo Atas (NSELOATAS) station. The analysis was carried out by observing the change in the position of the 2018 and 2019 regression lines against the theoretical lines of FAG and BCFAG, so it can be described as in Figure 4. In this study, the FAG value used is the theoretical FAG value, which is -0.308673 mGal/m (red line). The Bouguer effect used is the Bouguer infinity slab and the spherical Bouguer effect. For the Merapi area, if the density is assumed to be $\rho = 2,4 \text{ gr/cm}^3$ [8] then the theoretical gradient value for the effect of free air + infinity slab Bouguer (black line) is $\Delta g/\Delta h = -0.208 \text{ mGal/m}$; while the theoretical gradient value of free air + spherical Bouguer effect (yellow line) is obtained at $\Delta g/\Delta h = -0.242 \text{ mGal/m}$. From the processing results, the gradient value is obtained from the regression line equation $\Delta g_{obs}/\Delta h$ in 2018 and 2019. The regression line equation $\Delta g_{obs}/\Delta h$ in 2018 is obtained $\Delta g = -0,2727 \Delta h - 17,584$, while for 2019 the regression line equation $\Delta g = -0,2706 \Delta h - 17,754$. The gradient value of $\Delta g_{obs}/\Delta h$ in 2018 is greater than the gradient in 2019 with a very small difference value of 0.002 mGal/m . This shows that there is a very small change in density

caused by the volcanic activity of Merapi for the period 2018-2019.

In the case of volcanoes, [19] stated that the Bouguer spherical effect is more precise and realistic than the Bouguer infinity slab. Based on Figure 4, it can be seen that the gradients in 2018 and 2019 are closer to the theoretical gradient of the free air + spherical Bouguer effect.

Kelud Volcano:

With the similar process for Mount Kelud shown in Figure 5.

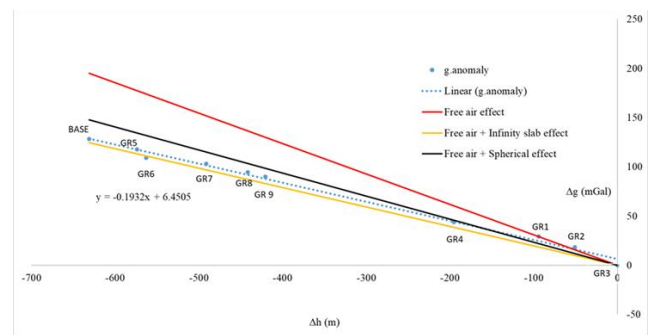


Figure 5 Graph of Δg_{obs} against Δh Kelud Volcano 2019

From the processing results obtained $\Delta g = -0,1932 \Delta h - 6,4505$. As in the case of Merapi Volcano, Kelud Volcano shows that the gradient is closer to the theoretical gradient of the free air + spherical Bouguer effect.

3.1 The Complete Bouguer Anomaly

The simple Bouguer effect correction is carried out without taking into account the topographic surface around the observation point. In reality, the surface around the observation point is not flat, but undulating. The existence of hills and valleys has not been taken into account in the simple Bouguer anomaly so it needs to be added. The process of adding the effects of the presence of hills and valleys can be done with terrain correction. A simple terrain-corrected Bouguer anomaly will produce a complete Bouguer anomaly.

Mount Merapi:

The complete Bouguer anomaly graph with the value of $= \Delta g_{obs} + \text{free air effect} - \text{infinity slab effect} + \text{Terrain effect}$ and the value of $= \Delta g_{obs} - \text{free air effect} + \text{spherical effect} + \text{terrain effect}$ with a first-order polynomial line equation approach can be seen in Figures 6 and 7; while the second-order line equation approach can be seen in Figures 8 and 9; and the third-order line equation approach can be seen in Figures 10 and 11.

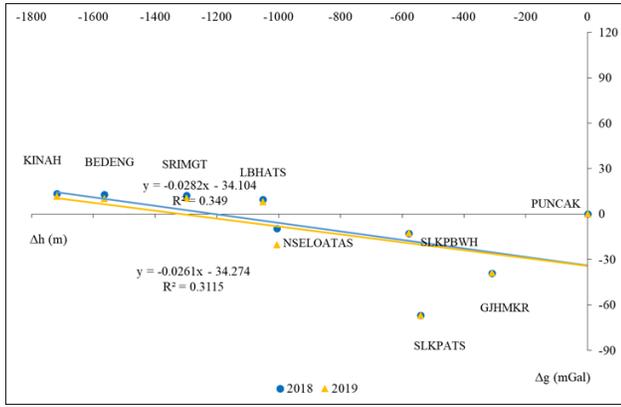


Figure 6 Complete Bouguer anomaly graph = Δg_{obs} + free air effect - infinity slab effect + terrain effect with a first-order polynomial line equation approach

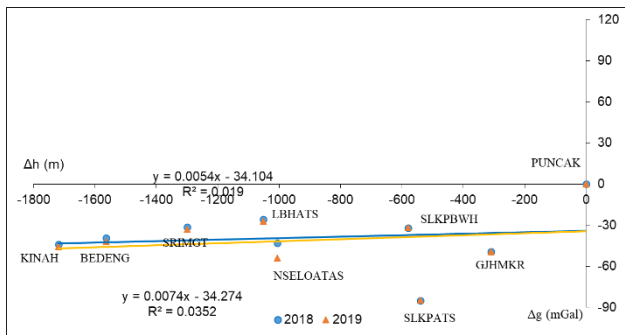


Figure 7 Complete Bouguer anomaly graph = Δg_{obs} - free air effect + spherical effect + terrain effect with a first-order polynomial line equation approach

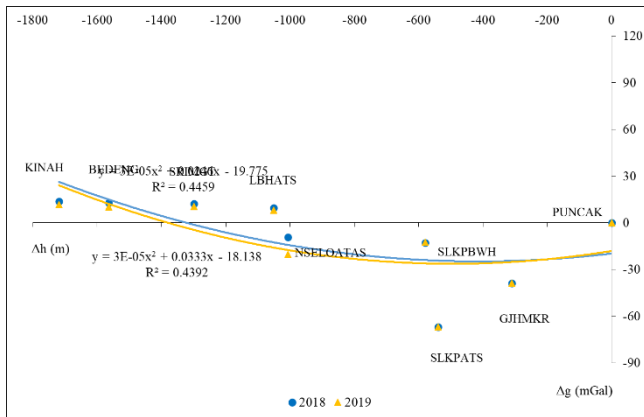


Figure 8 Complete Bouguer graph = Δg_{obs} + free air effect - infinity slab effect + terrain effect with a second order polynomial line equation approach

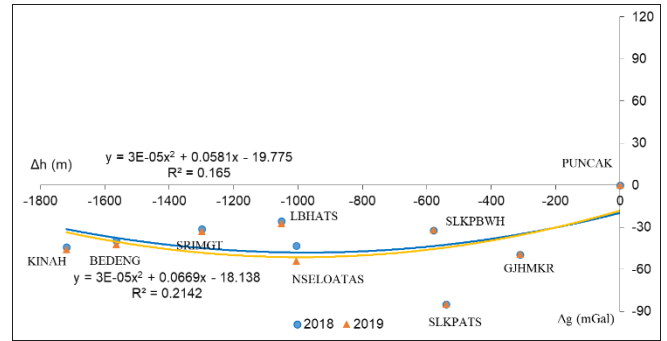


Figure 9 Complete Bouguer graph = Δg_{obs} - free air effect + spherical effect + terrain effect with a second order polynomial line equation approach

By analyzing the complete Bouguer anomaly, we assume that the resulting anomaly originates from within the body of Merapi Volcano. With a first-order or second-order polynomial approach, the coefficient of determination (R^2) is less than 50%, so it is not used to analyze only the third-order polynomial approach is used to analyze data on Merapi Volcano. The complete Bouguer Anomaly data for 2018 and 2019 with Bouguer correction in the form of an infinity slab has almost the same coefficient of determination of around 71.5%; while with Bouguer correction in the form of spherical effect the coefficient of determination is 59%.

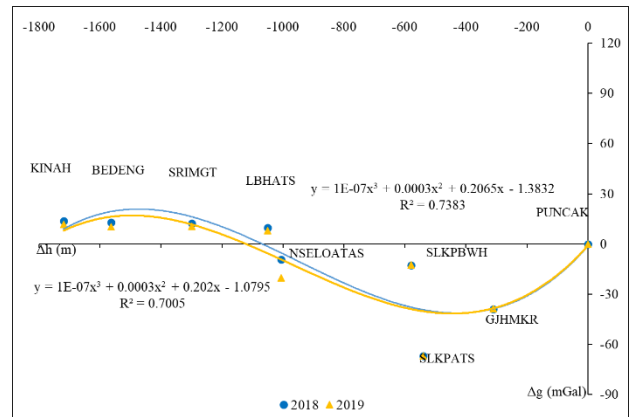


Figure 10 Complete Bouguer graph = Δg_{obs} + free air effect - infinity slab effect + terrain effect with a third-order polynomial line equation approach

The polynomial coefficients Δh_3 and Δh_2 , both corrected by the infinity slab and the spherical effect, show the same value. In this case, the gravity anomaly data from within the body of Merapi Volcano in 2018 and 2019 did not experience much change.

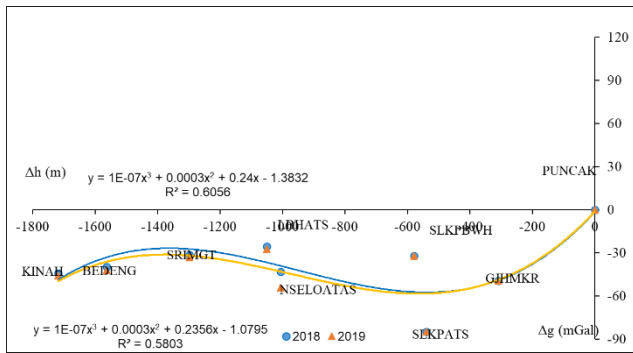


Figure 11 Complete Bouguer graph = Δg_{obs} - free air effect + spherical effect + terrain effect with a third-order polynomial line equation approach

Kelud Volcano:

The complete Bouguer anomaly graph with value = Δg_{obs} + free air effect - infinity slab + terrain and value = Δg_{obs} + free air effect - spherical effect + terrain with a first order polynomial line equation approach can be seen in Figures 12 and 13; while the second-order line equation approach can be seen in Figures 14 and 15; and the third-order line equation approach can be seen in Figures 16 and 17.

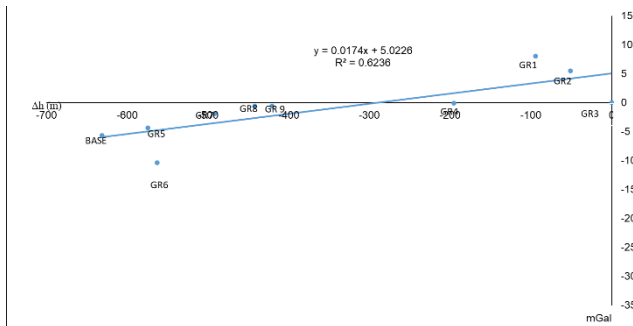


Figure 12 Complete Bouguer anomaly graph = Δg_{obs} + free air effect - infinity slab + terrain effect with a first-order line equation approach

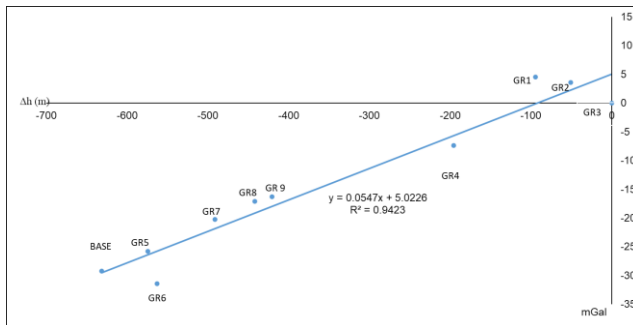


Figure 13 Complete Bouguer graph = Δg_{obs} + free air effect - spherical effect + terrain effect with a first order line equation approach

By analyzing the complete Bouguer anomaly like the analysis of Merapi Volcano, we assume that the

anomaly caused originates from within the body of Kelud Volcano. The first-order polynomial approach to third-order polynomial has a coefficient of determination (R^2) of more than 50%, so all of them are used to analyze Kelud Volcano data.

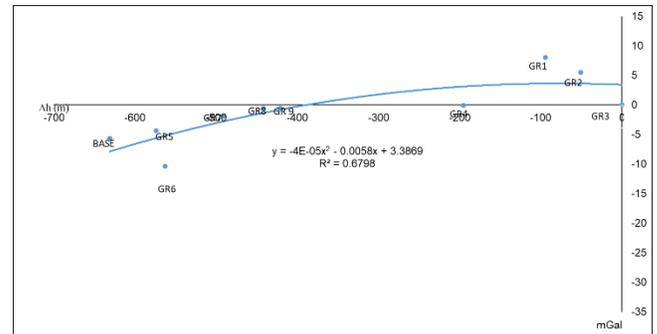


Figure 14 Complete Bouguer graph = Δg_{obs} + free air effect - infinity slab + terrain effect with a second order line equation approach

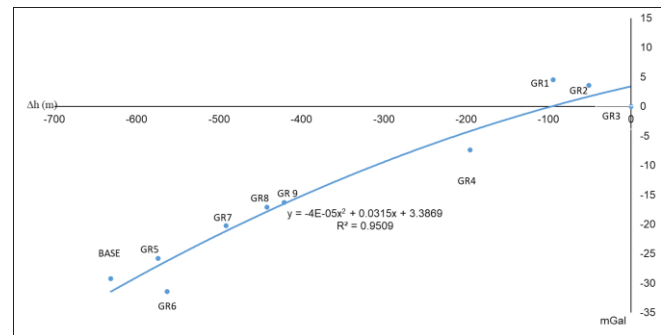


Figure 15 Complete Bouguer graph = Δg_{obs} + free air effect - spherical effect + terrain effect with a second order line equation approach

By approaching:

The first order polynomial equation, the complete Bouguer anomaly, the 2019 data with the Bouguer correction in the form of an infinity slab, has a coefficient of determination of 62%; while with Bouguer correction in the form of spherical effect the coefficient of determination is 94%. The polynomial coefficient h and the corrected constant with the infinity slab and the spherical effect are different.

The second order polynomial line equation, the complete Bouguer anomaly, the 2019 data with the Bouguer correction in the form of an infinity slab, has a coefficient of determination of 68 %; while with Bouguer correction in the form of spherical effect the coefficient of determination is 95%. The polynomial coefficient h_2 and the constant corrected by the infinity slab and the spherical effect show the same value.

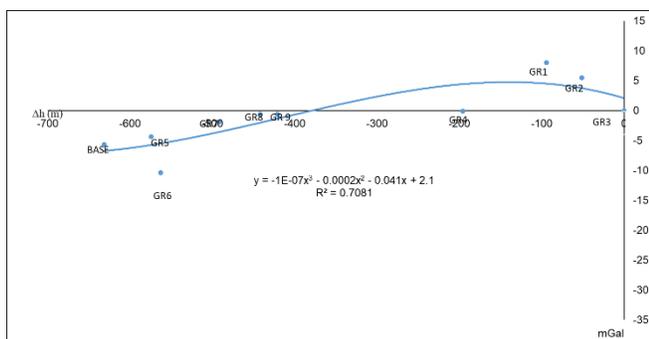


Figure 16 Complete Bouguer graph = Δg_{obs} + free air effect - infinity slab + terrain effect with a third-order line equation approach

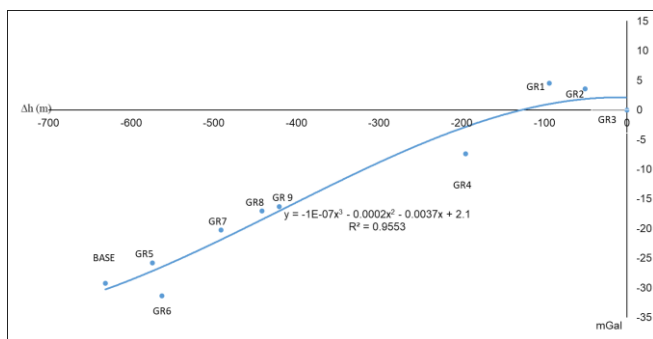


Figure 17 Complete Bouguer graph = Δg_{obs} + free air effect - spherical effect + terrain effect with a third-order line equation approach

The third order polynomial line equation, the complete Bouguer anomaly, the 2019 data with a Bouguer correction in the form of an infinity slab having a coefficient of determination of 71%; while with Bouguer correction in the form of spherical effect the coefficient of determination is 96%. The polynomial coefficients h_3 and h_2 the constants, both corrected by the infinity slab and the spherical effect, show the same values. The coefficient of determination for the complete Bouguer anomaly data for Kelud Volcano in 2019 with the Bouguer correction in the form of a spherical effect has a higher coefficient of determination (about 95%) compared to that corrected by the infinity slab (about 67%).

4.0 CONCLUSION

In this case, the gravity anomaly data from within the body of Merapi Volcano in 2018 and 2019 did not experience much change. The highest coefficient of determination (96%) for gravity anomaly data from inside the body of Kelud Volcano in 2019 is the Bouguer correction in the form of a spherical effect. Based on the equations of second order and third order polynomials, there are differences in the sign of the polynomial coefficients, for the data of Merapi Volcano the coefficient is opposite in sign to the data

of Kelud Volcano, this indicates that the internal source of the gravity anomaly from within the body of Merapi Volcano is different from the gravity anomaly from within the body of Kelud Volcano.

Conflicts of Interest

The author(s) declare(s) that there is no conflict of interest regarding the publication of this paper.

Acknowledgement

The author would like to thank FMIPA - UGM (Faculty of Mathematics and Natural Sciences -Gadjah Mada University) for providing the opportunity to participate in Lecturer Research Grants Department Of Physics the 2020 program with grant number: 99/J01.1.28/PL.06.02/2020. The authors also thank the Center for Research and Development of Geological Disaster Technology (BPPTKG) Yogyakarta for the secondary gravity data.

References

- [1] B. Voight, E. Constantine, S. Siswoidjoyo, and R. Torley. 2000. Historical Eruptions of Merapi Volcano, Central Java, Indonesia, 1768–1998. *Journal of Volcanology and Geothermal Research*. 100: 69-138. Doi: 10.1016/S0377-0273(00)00134-7.
- [2] M. R. Dove. 2008. Perception of Volcanic Eruption as Agent of Change on Merapi Volcano, Central Java. *Journal of Volcanology and Geothermal Research*. 172(3): 329-337. Doi: 10.1016/j.jvolgeores.2007.12.037.
- [3] R. Scandone, K. V. Cashman, and S. D. Malone. 2007. Magma Supply, Magma Ascent and the Style of Volcanic Eruptions. *Earth and Planetary Science Letters*. 253(3): 513-529. Doi: 10.1016/j.epsl.2006.11.016.
- [4] J. W. Esson. 1982. *Geodesy* (4th edn) by G. Bomford. Clarendon Press, Oxford. *Geological Journal*. 17(1): 66-67. Doi: 10.1002/gj.3350170108.
- [5] W. M. Telford, W. M. Telford, L. P. Geldart, R. E. Sheriff, and R. E. Sheriff. 1990. *Applied Geophysics*. Cambridge University Press.
- [6] D. L. Turcotte and G. Schubert. 2002. *Geodynamics*. 2nd Edition. Cambridge University Press.
- [7] D. Dzurisin. 2006. *Volcano Deformation*. Berlin, Heidelberg: Springer Berlin Heidelberg. Doi: 10.1007/978-3-540-49302-0.
- [8] P. Jousset, S. Dwipa, F. Beauducel, T. Duquesnoy, and M. Diament. 2000. Temporal Gravity at Merapi during the 1993–1995 Crisis: An Insight into the Dynamical Behaviour of Volcanoes. *Journal of Volcanology and Geothermal Research*. 100(1): 289-320. Doi: 10.1016/S0377-0273(00)00141-4.
- [9] D. Dzurisin. 2006. *Volcano Deformation*. Berlin, Heidelberg: Springer. Doi: 10.1007/978-3-540-49302-0.
- [10] A. Ratdomopurbo and G. Poupinet. 2000. An Overview of the Seismicity of Merapi Volcano (Java, Indonesia), 1983–1994. *Journal of Volcanology and Geothermal Research*, 100(1): 193-214. Doi: 10.1016/S0377-0273(00)00137-2.
- [11] A. Saepuloh, K. Koike, M. Omura, M. Iguchi, and A. Setiawan. 2010. SAR- and Gravity Change-based Characterization of the Distribution Pattern of Pyroclastic Flow Deposits at Mt. Merapi during the Past 10 years. *Bull Volcanol*. 72(2): 221-232. Doi: 10.1007/s00445-009-0310-x.

- [12] C. Tiede, A. G. Camacho, C. Gerstenecker, J. Fernández, and I. Suyanto. 2005. Modeling the Density at Merapi Volcano Area, Indonesia, via the Inverse Gravimetric Problem. *Geochemistry, Geophysics, Geosystems*. 6(9). Doi: 10.1029/2005GC000986.
- [13] Blake, D. M., Wilson, G., Stewart, C., Craig, H. M., Hayes, J. L., Jenkins, S. F., Wilson, T. M., Horwell, C. J., Andreastuti, S., Daniswara, R., Ferdiwijaya, D., Leonard, G. S., Hendrasto, M., and Cronin, S. 2015. The 2014 Eruption of Kelud Volcano, Indonesia: Impacts on Infrastructure, Utilities, Agriculture and Health. GNS Science Report 2015/15.
- [14] L. R. Goode, H. K. Handley, S. J. Cronin, and M. Abdurrachman. 2019. Insights into Eruption Dynamics from the 2014 Pyroclastic Deposits of Kelut Volcano, Java, Indonesia, and Implications for Future Hazards. *Journal of Volcanology and Geothermal Research*. 382: 6-23. Doi: 10.1016/j.jvolgeores.2018.02.005.
- [15] S. Hidayati et al. 2019. Differences in the Seismicity Preceding the 2007 and 2014 Eruptions of Kelud Volcano, Indonesia. *Journal of Volcanology and Geothermal Research*. 382: 50-67. Doi: 10.1016/j.jvolgeores.2018.10.017.
- [16] U. Sumotarto. 2018. Geothermal Energy Potential of Arjuno and Welirang Volcanoes Area, East Java, Indonesia. *International Journal of Renewable Energy Research (IJRER)*. 8(1): Art. no. 1.
- [17] M. F. Kane. 1962. A Comprehensive System of Terrain Corrections using a Digital Computer. *Geophysics*. 27(4): 455-462. Doi: 10.1190/1.1439044.
- [18] D. Nagy. 1966. The Prism Method for Terrain Corrections using Digital Computers. *PAGEOPH*. 63(1): 31-39. Doi: 10.1007/BF00875156.
- [19] G. Williams-Jones and H. Rymer. 2002. Detecting Volcanic Eruption Precursors: A New Method using Gravity and Deformation Measurements. *Journal of Volcanology and Geothermal Research*. 113. Doi: 10.1016/S0377-0273(01)00272-4.
- [19] BPPTKG. 2018. Karakteristik Gunung Merapi. URL (accessed 11.13.19).
- [20] www.tides.big.go.id.